Progress In Electromagnetics Research C, Vol. 94, 119–130, 2019

HF Skywave Polarized MIMO Channels with Oblique One-Hop Paths

Umaisaroh Umaisaroh[1], Gamantyo Hendrantoro[1, *], and Varuliantor Dear[2]

Abstract—The presence of the O and X modes in the HF skywave propagation has previously been investigated experimentally for their role in providing polarization diversity and improving channel capacity when a MIMO structure is employed. A mathematical treatment of MIMO channel modelling and capacity improvement has also been reported but limited to NVIS links only. This paper reports the mathematical derivation of the HF 2×2 polarized MIMO channels when cross-dipoles, i.e., a pair of orthogonally polarized horizontally-oriented dipoles, are used at both ends to examine the cross-polarization property and capacity improvement factor (CIF), with the transmitter-receiver range being near enough to allow single-hop paths only but also distant enough to make the trajectory oblique. Results on the cross-polarization property suggest that the power contributions of the waves from the two transmitters that arrive at each receiver are equal. In addition, the signal from any one of the transmitters is received by the two receivers with unbalanced powers that depend on the phase shift difference between the O and X paths. It is also observed that on average the MIMO channels with oblique paths have lower capacity than the NVIS MIMO channels due to the reduced orthogonality between polarizations of antennas in the dual-antenna system at each end. The above hypotheses are confirmed through ray-tracing simulation and field measurement over a 575 km HF radio link.

1. INTRODUCTION

High Frequency (HF) skywave communication systems in the 3–30 MHz frequency range have been considered by many as an option for emergency communication or an access technology for remote areas, which is less costly and more robust than satellite-based or other terrestrial systems, especially due to their capability to reach a very long distance by means of ionospheric reflections [1, 2]. In emergency situations, sometimes it is necessary to send large files or data over the HF channels, thereby requiring more capacity of the channels. Due to its low frequency and for frequency division multiplexing purposes, the HF radio channels have a limited useable bandwidth, i.e., 3–20 kHz [3], which in turn limits the rate of information that can be delivered over the channels. Multiple-input multiple-output (MIMO) antenna structure has been considered to improve channel capacity, not only in terrestrial wireless channels [4, 5] but also in HF skywave channels [6–8].

In the last decade, researchers have recognized the importance of the characteristic waves, the extraordinary (X) and ordinary (O), that in general are elliptically polarized with opposite senses, in realizing polarization diversity and HF skywave MIMO communications without the need of large spacing between antennas [7–14]. While [7–10] discover, by simulation and experiment, a lower correlation among subchannels and a greater capacity gain over SISO channels when an antenna structure with two complementary circular polarizations is used compared to a system with linearly polarized antennas, [14] shows mathematically that linearly-polarized antennas can achieve polarization diversity.

Received 27 April 2019, Accepted 3 July 2019, Scheduled 17 July 2019
* Corresponding author: Gamantyo Hendrantoro (gamantyo@ee.its.ac.id).
[1] Department of Electrical Engineering, Institut Teknologi Sepuluh Nopember, Indonesia. [2] Space Science Center, National Institute of Aeronautics and Space (LAPAN), Indonesia.

If an implementation over a local area of up to a 200 km radius is desired, NVIS propagation with almost 90° elevation angles can be exploited [12]. However, for wider coverage area, the path of the radio waves should take a slanted elevation angle. In a single-hop radio wave transmission through the ionosphere, the elevation angle varies with the ground range between the transmitter and receiver. As the paths become oblique, the orthogonally polarized horizontal antennas do not appear as orthogonal as in NVIS case for the departing and arriving waves, which cause differences in MIMO capacity. This paper shows that oblique paths reduce the capacity gain relative to the SISO capacity due to the decreasing orthogonality between the cross-dipoles.

In addition, the natural presence of the O and X modes in HF skywave channels means that, unlike terrestrial polarized MIMO wireless channels in which there is little cross-polar leakage [5], there can be large cross-polarization in MIMO HF skywave channels. This further implies that horizontal cross-dipoles at the transmitter and receiver can be deployed with different, arbitrary azimuth orientations, although the impact of radiation pattern of the horizontal dipole at inclined elevations will take effect for oblique paths. Hence, the elevation angle and the azimuth alignment angle between the cross-dipole structure and the transmitter-receiver axis are equally important parameters of the MIMO channel and are taken into account in the channel modelling herein.

In this paper, mathematical derivation of HF MIMO channel matrix for relatively short distance, i.e., one-hop, oblique propagation paths using linearly polarized antennas is presented. Experimental results with cross-dipoles on a 575 km path length between two locations, Bandung and Surabaya, in the equatorial region of Indonesia shows the capacity improvement of 1.49–1.79, while simulation results give higher improvement, in the range 1.73–1.88. Both the mathematical treatment and experiment reveal the behavior of HF polarized MIMO channels, including the power transition matrix, diversity phenomenon, the capacity improvement over SISO channels, and the effect of oblique paths on the capacity improvement. In summary, the main contribution of this paper includes:

(i) The expression of the oblique single-hop HF polarized MIMO channels, which differs from the NVIS case primarily in the dependence of the channel on the elevation angle of the O and X waves. With the adoption of vectors that express the orientation of the MIMO antennas at both sides with respect to the transmitter-receiver axis, this becomes a more general expression of the skywave polarized MIMO channels.

(ii) The expression and its experimental proof of the cross-polarization in the form of power transition matrix between the transmit and receive antennas for a simplified condition, which reveals that there is a tendency of power unbalance between the two receive antennas in HF oblique skywave MIMO channels, whose extent depends on the phase shift difference of the O and X waves. On the other hand, for each receive antenna the power contributions from the two transmit antennas tend to be equal. These observations have not been pointed out in [14] but are in line with the result in [13].

(iii) The experimental proof that on average the capacity improvement factor (CIF) of the oblique skywave MIMO channels over SISO channels is lower than the CIF of the NVIS MIMO channels, owing to the lower orthogonality of the cross-dipoles for waves with oblique trajectories.

2. CHANNEL MODEL

2.1. The HF Polarized MIMO Channels

In this section, firstly we attempt to formulate the 2×2 MIMO HF channels with oblique paths when the dual-transmitter and dual-receiver systems use horizontal cross-dipoles with different orientations, making an azimuth difference φ. As illustrated in Figure 1, when the radio waves penetrate the ionospheric magnetoplasma, each of them splits into the RHCP and LHCP components that propagate in the X and O modes, respectively, and bend down towards the ground.

Suppose that two different signals, expressed herein in their respective low-pass equivalents, are transmitted respectively by the two co-located antennas. Also suppose that $\mathbf{x}$ and $\mathbf{y}$ are the unit vectors describing antenna polarizations. The signal transmitted by the first antenna T1 having gain pattern

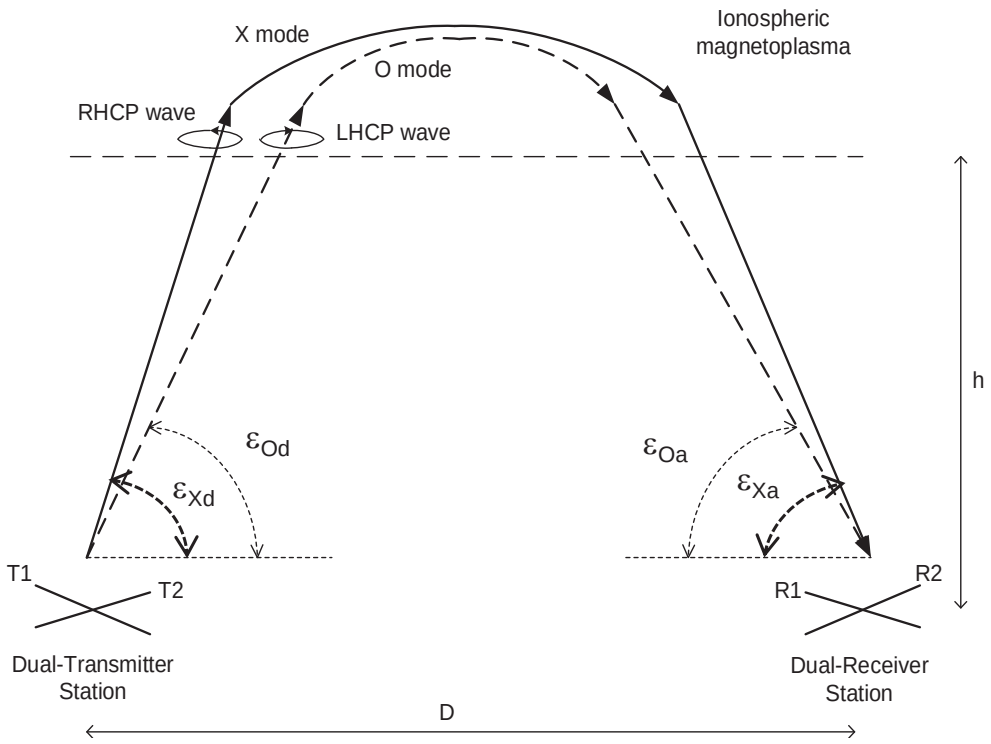

Figure 1. Illustration of the HF skywave polarized MIMO system.

of g_{T1} is:

$$\begin{aligned}\mathbf{E}_1 =& s_1 g_{\mathrm{T1}}(\varepsilon_{\mathrm{d}})\mathbf{x} \\ =& \frac{1}{2}s_1 g_{\mathrm{T1}}(\varepsilon_{\mathrm{d}})(\mathbf{x} - j\mathbf{y}) + \frac{1}{2}s_1 g_{\mathrm{T1}}(\varepsilon_{\mathrm{d}})(\mathbf{x} + j\mathbf{y})\end{aligned} \tag{1}$$

where s_1 denotes the low-pass equivalent signal, and g_{T1} denotes the field pattern of the T1 antenna at the elevation angle of departure, ε_{d}. The second row describes the RHCP and LHCP forms [15], respectively. Similarly, the second antenna T2 transmits:

$$\begin{aligned}\mathbf{E}_2 =& s_2 g_{\mathrm{T2}}(\varepsilon_{\mathrm{d}})\mathbf{y} \\ =& \frac{1}{2}s_2 g_{\mathrm{T2}}(\varepsilon_{\mathrm{d}})(j\mathbf{x} + \mathbf{y}) + \frac{1}{2}s_2 g_{\mathrm{T2}}(\varepsilon_{\mathrm{d}})(-j\mathbf{x} + \mathbf{y})\end{aligned} \tag{2}$$

where the symbols are of similar definitions to those in the previous equation.

We assume that a transmit station employs two transmitters and two horizontal antennas with orthogonal linear polarizations in directions $\mathbf{x}$ and $\mathbf{y}$, unit vectors spanning the horizontal plane with $\mathbf{z}$ being the unit vector in vertical direction. The antennas are centered at the origin O. Suppose that transmitted radio waves leave the two antennas at azimuth α with respect to $\mathbf{x}$ following right hand rule and elevation ε with respect to the horizontal plane. Then unit vector $\mathbf{r}$ at the direction of wave departure can be generally expressed as:

$$\mathbf{r} = a\mathbf{x} + b\mathbf{y} + c\mathbf{z} \tag{3}$$

where

$$\begin{aligned}\sqrt{a^2 + b^2 + c^2} &= 1 \\ a = \sin\left(\frac{\pi}{2} - \varepsilon\right)\cos\alpha &= \cos\varepsilon\cos\alpha \\ b = \sin\left(\frac{\pi}{2} - \varepsilon\right)\sin\alpha &= \cos\varepsilon\sin\alpha \\ c = \cos\left(\frac{\pi}{2} - \varepsilon\right) &= \sin\varepsilon\end{aligned}$$

so that

$$\mathbf{r} = \mathbf{x}\cos\varepsilon\cos\alpha + \mathbf{y}\cos\varepsilon\sin\alpha + \mathbf{z}\sin\varepsilon \tag{4}$$

If vectors $\mathbf{p}_1$ and $\mathbf{p}_2$ are orthonormal, and both are orthogonal to vector $\mathbf{r}$ in the departure direction, there are many choices available for $\mathbf{p}_1$ and $\mathbf{p}_2$. In this example we can choose:

$$\mathbf{p}_1 = \frac{\left(\dfrac{\mathbf{x}}{a} - \dfrac{\mathbf{y}}{b}\right)}{\sqrt{\dfrac{1}{a^2} + \dfrac{1}{b^2}}} = \frac{b\mathbf{x} - a\mathbf{y}}{\sqrt{a^2+b^2}} \tag{5}$$

$$\mathbf{p}_2 = \mathbf{r} \times \mathbf{p}_1 = \frac{ac\mathbf{x} + bc\mathbf{y} - (a^2+b^2)\mathbf{z}}{\sqrt{a^2+b^2}} \tag{6}$$

Projections of $\mathbf{E}_1$ and $\mathbf{E}_2$ onto the plane normal to $\mathbf{r}$, the direction of propagation, can be expressed, respectively, as:

$$\begin{aligned}\mathbf{E}_{1\mathrm{p}} &= (\mathbf{E}_1 \cdot \mathbf{p}_1)\,\mathbf{p}_1 + (\mathbf{E}_1 \cdot \mathbf{p}_2)\,\mathbf{p}_2 \\ &= \frac{s_1 g_{\mathrm{T}1}}{a^2+b^2}\left[(a^2c^2+b^2)\mathbf{x} + (abc^2-ab)\mathbf{y} - ac(a^2+b^2)\mathbf{z}\right]\end{aligned} \tag{7}$$

$$\begin{aligned}\mathbf{E}_{2\mathrm{p}} &= (\mathbf{E}_2 \cdot \mathbf{p}_1)\,\mathbf{p}_1 + (\mathbf{E}_2 \cdot \mathbf{p}_2)\,\mathbf{p}_2 \\ &= \frac{s_2 g_{\mathrm{T}2}}{a^2+b^2}\left[(abc^2-ab)\mathbf{x} + (a^2+b^2c^2)\mathbf{y} - bc(a^2+b^2)\mathbf{z}\right]\end{aligned} \tag{8}$$

where the symbols are of similar definitions to those in previous equation.

These projected vectors are, unlike the original ones, correlated to some extent depending on the elevation angle. There are two conditions that make the projected vectors orthogonal, which is indicated by both $\mathbf{E}_{1\mathrm{p}}$ and $\mathbf{E}_{2\mathrm{p}}$ being non-zero while their dot product is zero: (i) Both a and b are zero, i.e., the NVIS condition. (ii) Only one of them is zero, which happens when one of the antennas is in line with the departure path along the transmitter-receiver axis. However, it should be noted that if the receiver cross-dipole system is a rotated copy of the transmitter's (by an angle later denoted by φ), then there will be loss of orthogonality at the receiving side.

When the linearly-polarized waves enter the ionospheric magnetoplasma, each wave splits into two characteristic modes having two elliptical polarizations with opposite senses of rotation, i.e., the O and X modes. Following an assumption of more ideal situation, in our derivation the $\mathbf{x}$ and $\mathbf{y}$ vectors are expressed in orthogonal circularly-polarized components, instead of elliptically-polarized ones [9]:

$$\mathbf{x} = \frac{1}{2}\left[(\mathbf{x} - j\mathbf{y}) + (\mathbf{x} + j\mathbf{y})\right] \tag{9}$$

$$\mathbf{y} = -j\frac{1}{2}\left[(\text{-}\mathbf{x} + j\mathbf{y}) + (\mathbf{x} + j\mathbf{y})\right] \tag{10}$$

In the above, the first and second terms of each equation represent the right-hand circularly polarized (RHCP) and left-hand circularly polarized (LHCP) components, corresponding to the sense of rotation of X and O modes, respectively. Subsequently, the waves propagating along $\mathbf{r}$ can now be rewritten as:

$$\begin{aligned}\mathbf{E}_{1\mathrm{p}} &= \frac{s_1 g_{\mathrm{T}1}}{a^2+b^2}\left[\frac{1}{2}(a^2c^2+b^2)[(\mathbf{x} - j\mathbf{y}) + (\mathbf{x} + j\mathbf{y})\right] \\ &\quad -j\frac{1}{2}\left[(abc^2-ab)[(\text{-}\mathbf{x} + j\mathbf{y}) + (\mathbf{x} + j\mathbf{y})] - ac(a^2+b^2)\mathbf{z}\right]\end{aligned} \tag{11}$$

$$\begin{aligned}\mathbf{E}_{2\mathrm{p}} &= \frac{s_2 g_{\mathrm{T}2}}{a^2+b^2}\left[\frac{1}{2}(abc^2-ab)[(\mathbf{x} - j\mathbf{y}) + (\mathbf{x} + j\mathbf{y})\right] \\ &\quad -j\frac{1}{2}(a^2+b^2c^2)\left[(\text{-}\mathbf{x} + j\mathbf{y}) + (\mathbf{x} + j\mathbf{y})\right] - bc(a^2+b^2)\mathbf{z}\right]\end{aligned} \tag{12}$$

Grouping the RHCP and LHCP components from the two waves, we obtain:

$$\begin{aligned}\mathbf{E}_{\mathrm{R}} &= \mathbf{E}_{1\mathrm{pR}} + \mathbf{E}_{2\mathrm{pR}} \\ &= \left[\frac{1}{2}\frac{s_1 g_{\mathrm{T1}}}{a^2+b^2}[(a^2c^2+b^2)+j(abc^2-ab)] + \frac{1}{2}\frac{s_2 g_{\mathrm{T2}}}{a^2+b^2}[(abc^2-ab)+j(a^2+b^2c^2)]\right](\mathbf{x}-j\mathbf{y}) \quad (13)\end{aligned}$$

$$\begin{aligned}\mathbf{E}_{\mathrm{L}} &= \mathbf{E}_{1\mathrm{pL}} + \mathbf{E}_{2\mathrm{pL}} \\ &= \left[\frac{1}{2}\frac{s_1 g_{\mathrm{T1}}}{a^2+b^2}\left[(a^2c^2+b^2)-j(abc^2-ab)\right] + \frac{1}{2}\frac{s_2 g_{\mathrm{T2}}}{a^2+b^2}[(abc^2-ab)-j(a^2+b^2c^2)]\right](\mathbf{x}+j\mathbf{y}) \quad (14)\end{aligned}$$

At the receiving station, the two-antenna system is a rotated version with respect to the transmit antenna system with rotation angle of φ. It means that if there is no change in the course of the propagation with respect to the xy plane, the arrival azimuth with respect to the receive antenna system is $\alpha+\varphi$. Accordingly, the linear polarizations of the two receive antennas become $\mathbf{x}\cos\varphi+\mathbf{y}\sin\varphi$ and $\mathbf{x}\sin\varphi+\ \mathbf{y}\cos\varphi$. However, for simplicity we assume $\varphi=0$.

The RHCP and LHCP components of the two transmit signals from Eqs. (**??**) and (12) can be grouped and arranged into a transmit matrix $\mathbf{G}_{\mathrm{T}}$:

$$\mathbf{G}_{\mathrm{T}} = \frac{1}{2}\begin{bmatrix} g_{\mathrm{T1}}(\varepsilon_{\mathrm{Xd}}) & g_{\mathrm{T2}}(\varepsilon_{\mathrm{Xd}}) \\ g_{\mathrm{T1}}(\varepsilon_{\mathrm{Od}}) & g_{\mathrm{T2}}(\varepsilon_{\mathrm{Od}})\end{bmatrix} \quad (15)$$

where the departure elevations for the wave components that later follow the X and O modes are $\varepsilon_{\mathrm{Xd}}$ and $\varepsilon_{\mathrm{Od}}$, respectively.

The RHCP component of the waves experiences the X propagation mode, whereas the LHCP component propagates through the O mode. Herein we model the resulting channel as frequency-flat, under the assumption that the delay spread incurred by the different modes is much lower than the transmitted symbol period. Hence, the channel responses for the X and O modes, respectively, can be arranged in a diagonal matrix:

$$\mathbf{H}_{\mathrm{OX}} = \begin{bmatrix} \gamma_{\mathrm{X}} e^{-j\theta_{\mathrm{X}}}(\mathbf{x}-j\mathbf{y}) & 0 \\ 0 & \gamma_{\mathrm{O}} e^{-j\theta_{\mathrm{O}}}(\mathbf{x}+j\mathbf{y})\end{bmatrix} \quad (16)$$

where γ_{X} and γ_{O} denote the gain factors and θ_{X} and θ_{O} the phase shifts of the responses for the X and O propagation modes, respectively.

Due to down-bending of the incoming waves back toward the earth by the ionospheric layer, there are also changes in direction of vectors of the electric field (i.e., polarization). Hence, for the waves propagating downward from the ionosphere we use **x'** and **y'** to denote the result of wave bending on $\mathbf{x}$ and $\mathbf{y}$, where

$$\mathbf{x'} = \mathbf{x}\sin\alpha - \mathbf{y}\cos\alpha \quad (17)$$

$$\mathbf{y'} = -\mathbf{x}\cos\alpha - \mathbf{y}\sin\alpha \quad (18)$$

Therefore, the channel response matrix in Eq. (16) can be written as Eq. (19):

$$\check{\mathbf{H}}_{\mathrm{OX}} = \begin{bmatrix} \gamma_{\mathrm{X}} e^{-j\theta_{\mathrm{X}}}(\mathbf{x'}-j\mathbf{y'}) & 0 \\ 0 & \gamma_{\mathrm{O}} e^{-j\theta_{\mathrm{O}}}(\mathbf{x'}+j\mathbf{y'})\end{bmatrix} \quad (19)$$

By assuming that receive antennas are aligned with $\mathbf{x}$ and $\mathbf{y}$, the waves arriving at the co-located receive antennas after passing through the X and O propagation modes can be expressed in matrix form:

$$\mathbf{G}_{\mathrm{R}} = \begin{bmatrix} g_{\mathrm{R1}}(\varepsilon_{\mathrm{Xa}})\mathbf{x} & g_{\mathrm{R1}}(\varepsilon_{\mathrm{Oa}})\mathbf{x} \\ g_{\mathrm{R2}}(\varepsilon_{\mathrm{Xa}})\mathbf{y} & g_{\mathrm{R2}}(\varepsilon_{\mathrm{Oa}})\mathbf{y}\end{bmatrix} \quad (20)$$

where $\varepsilon_{\mathrm{Oa}}$ and $\varepsilon_{\mathrm{Xa}}$ denote elevation angles of arrival of the O and X waves, respectively, and g_{R1} and g_{R2} denote gain patterns of the receive antennas.

The 2×2 MIMO channel matrix can then be written as:

$$\mathbf{H} = \mathbf{G}_{\mathrm{R}} \check{\mathbf{H}}_{\mathrm{OX}} \mathbf{G}_{\mathrm{T}} \tag{21}$$

It should be noted that the matrix multiplication involves dot products between spatial vectors $\mathbf{x}$ and $\mathbf{y}$ contained in the elements of $\mathbf{G}_{\mathrm{T}}$ and $\mathbf{G}_{\mathrm{R}}$. Subsequently, by writing the elements of $\mathbf{H}$ in Eqs. (21) into (22), the MIMO channel matrix elements are found to be:

$$\mathbf{H} = \begin{bmatrix} h_{11} & h_{12} \\ h_{21} & h_{22} \end{bmatrix} \tag{22}$$

where $h_{11} = \frac{1}{2}\left[g_{\mathrm{T1}}(\varepsilon_{\mathrm{Xd}}) g_{\mathrm{R1}}(\varepsilon_{\mathrm{Xa}})(\sin\alpha + j\cos\alpha)\gamma_{\mathrm{X}} e^{-j\theta_X} + g_{\mathrm{T1}}(\varepsilon_{\mathrm{Od}}) g_{\mathrm{R1}}(\varepsilon_{\mathrm{Oa}})(\sin\alpha - j\cos\alpha)\gamma_{\mathrm{O}} e^{-j\theta_O}\right]$
$h_{12} = \frac{1}{2}\left[g_{\mathrm{T2}}(\varepsilon_{\mathrm{Xd}}) g_{\mathrm{R1}}(\varepsilon_{\mathrm{Xa}})(\sin\alpha + j\cos\alpha)\gamma_{\mathrm{X}} e^{-j\theta_X} + g_{\mathrm{T2}}(\varepsilon_{\mathrm{Od}}) g_{\mathrm{R1}}(\varepsilon_{\mathrm{Oa}})(\sin\alpha - j\cos\alpha)\gamma_{\mathrm{O}} e^{-j\theta_O}\right]$
$h_{21} = \frac{1}{2}\left[g_{\mathrm{T1}}(\varepsilon_{\mathrm{Xd}}) g_{\mathrm{R2}}(\varepsilon_{\mathrm{Xa}})(-\cos\alpha + j\sin\alpha)\gamma_{\mathrm{X}} e^{-j\theta_X} + g_{\mathrm{T1}}(\varepsilon_{\mathrm{Od}}) g_{\mathrm{R2}}(\varepsilon_{\mathrm{Oa}})(-\cos\alpha - j\sin\alpha)\gamma_{\mathrm{O}} e^{-j\theta_O}\right]$
$h_{22} = \frac{1}{2}\left[g_{\mathrm{T2}}(\varepsilon_{\mathrm{Xd}}) g_{\mathrm{R2}}(\varepsilon_{\mathrm{Xa}})(-\cos\alpha + j\sin\alpha)\gamma_{\mathrm{X}} e^{-j\theta_X} + g_{\mathrm{T2}}(\varepsilon_{\mathrm{Od}}) g_{\mathrm{R2}}(\varepsilon_{\mathrm{Oa}})(-\cos\alpha - j\sin\alpha)\gamma_{\mathrm{O}} e^{-j\theta_O}\right]$

Alternatively, Eq. (21) can be rewritten as multiplication of matrices not containing the spatial vectors:

$$\mathbf{H} = \hat{\mathbf{G}}_{\mathrm{R}} \hat{\mathbf{H}}_{\mathrm{OX}} \hat{\mathbf{G}}_{\mathrm{T}} \tag{23}$$

where

$$\hat{\mathbf{G}}_{\mathrm{T}} = \frac{1}{2}\begin{bmatrix} g_{\mathrm{T1}}(\varepsilon_{\mathrm{Xd}}) & g_{\mathrm{T2}}(\varepsilon_{\mathrm{Xd}}) \\ g_{\mathrm{T1}}(\varepsilon_{\mathrm{Od}}) & g_{\mathrm{T2}}(\varepsilon_{\mathrm{Od}}) \end{bmatrix}$$

$$\hat{\mathbf{H}}_{\mathrm{OX}} = \begin{bmatrix} (\sin\alpha + j\cos\alpha)\gamma_{\mathrm{X}} e^{-j\theta_{\mathrm{X}}} & 0 \\ 0 & (\sin\alpha - j\cos\alpha)\gamma_{\mathrm{O}} e^{-j\theta_{\mathrm{O}}} \end{bmatrix}$$

$$\hat{\mathbf{G}}_{\mathrm{R}} = \begin{bmatrix} g_{\mathrm{R1}}(\varepsilon_{\mathrm{Xa}}) & g_{\mathrm{R1}}(\varepsilon_{\mathrm{Oa}}) \\ j g_{\mathrm{R2}}(\varepsilon_{\mathrm{Xa}}) & -j g_{\mathrm{R2}}(\varepsilon_{\mathrm{Oa}}) \end{bmatrix}$$

The $\hat{\mathbf{H}}_{\mathrm{OX}}$ matrix includes both the channel responses for the O and X modes and the vector associated with the impact of the down-bending by the ionospheric layer.

Then vector v of the received signals can be given as:

$$\mathbf{v} = \mathbf{H}\mathbf{s} + \mathbf{n} \tag{24}$$

where vector $\mathbf{v} = [v_1, v_2]^{\mathrm{T}}$ implicitly takes into account dot products of the received antenna polarizations and the corresponding linear vector components of the circularly polarized waves, while $\mathbf{s} = [s_{1\mathrm{p}}, s_{2\mathrm{p}}]^{\mathrm{T}}$ denotes the transmitted signals by the first and second antennas, respectively, in complex baseband form, and $\mathbf{n}$ denotes the complex baseband noise vector.

It can be seen in Eq. (22) that each SISO channel consists of two terms, representing the RHCP and LHCP components, respectively, a single-hop path originating from one of the transmit antennas and arriving at one of the antennas at the receiving side. The presence of both components with orthogonal polarizations indicates a naturally-induced diversity inherent in HF MIMO systems, which is responsible for the improvement in channel capacity because the MIMO structure nearly doubles the capacity of SISO systems.

Every element in Eq. (22) is the sum of two complex terms representing the contribution of the X and O modes, which, as noted before, does not happen in terrestrial wireless systems with polarized MIMO antenna structures, each consisting of random variables. For example, in each element the elevation angles of departure and arrival for the RHCP and LHCP waves vary with ionospheric condition, so are the range-dependent gain factors. However, as the case in terrestrial multipath fading channels [5], the largest variation of each of the sums originates from the random phase shift, for which an incremental distance of propagation in the order of half wavelength, e.g., 30 meters at 6 MHz, is enough to cause phase reversal to the propagating wave. Since the difference in path lengths between two terms in each of the sums depends on the ionospheric condition and can be arbitrary, it is safe to assume that the phase shifts are uniformly distributed between 0 and 2π.

2.2. Cross-Polarization

By assuming that the transmitter-receiver axis is in line with one of the dipoles at both sides, i.e., $\alpha = 0$, the extent of cross-polarization of the waves can be studied. Starting from the channel matrix in Eq. (22), the square magnitude of each SISO element can be derived.

In order to get an insight into what happens to the waves of orthogonal linear polarizations when they travel through the ionosphere, a reasonable simplification can be made by assuming that $\varepsilon_{\mathrm{X}} = \varepsilon_{\mathrm{O}}$, so that $g_{\mathrm{T1}}(\varepsilon_{\mathrm{X}}) = g_{\mathrm{T1}}(\varepsilon_{\mathrm{O}}) = g_{\mathrm{T1}}$, $g_{\mathrm{T2}}(\varepsilon_{\mathrm{X}}) = g_{\mathrm{T2}}(\varepsilon_{\mathrm{O}}) = g_{\mathrm{T2}}$, $g_{\mathrm{R1}}(\varepsilon_{\mathrm{X}}) = g_{\mathrm{R1}}(\varepsilon_{\mathrm{O}}) = g_{\mathrm{R1}}$, $g_{\mathrm{R2}}(\varepsilon_{\mathrm{X}}) = g_{\mathrm{R2}}(\varepsilon_{\mathrm{O}}) = g_{\mathrm{R2}}$, and $\gamma_{\mathrm{X}} \approx \gamma_{\mathrm{O}}$. However, we keep $\theta_{\mathrm{X}} \neq \theta_{\mathrm{O}}$, following the discussion on the independence of the phase shifts on the two modes. It can be found,

$$\frac{|h_{11}|^2}{|h_{21}|^2} = \frac{1 - \cos(\theta_{\mathrm{X}} - \theta_{\mathrm{O}})}{1 + \cos(\theta_{\mathrm{X}} - \theta_{\mathrm{O}})} \tag{25}$$

$$\frac{|h_{22}|^2}{|h_{12}|^2} = \frac{1 + \cos(\theta_{\mathrm{X}} - \theta_{\mathrm{O}})}{1 - \cos(\theta_{\mathrm{X}} - \theta_{\mathrm{O}})} \tag{26}$$

$$\frac{|h_{22}|^2}{|h_{21}|^2} = \frac{|h_{11}|^2}{|h_{12}|^2} = 1 \tag{27}$$

From Eq. (27) it can be seen that $|h_{22}|^2/|h_{21}|^2$ and $|h_{11}|^2/|h_{12}|^2$ are both equal to unity, although deviation from unity is expected in reality. This suggests that the power contributions of the waves from the two transmitters that arrive at each receiver are nearly equal.

On the other hand, Eqs. (25) and (26) indicate that when the radio wave transmitted from any one of the transmitters splits into two components arriving at the two receivers, the power ratio between them depends on the phase shift difference between the X and O paths, with a unit power ratio occurring for phase shift difference of $\pm\pi/2$. As a result, h_{11} and h_{12} have similar power gains, so do h_{22} and h_{21}, but the two pairs might individually have different power gain ratios. The power transition matrix between the two transmitters and two receivers can be expressed as

$$\Gamma = \begin{bmatrix} \frac{1}{2}\left(1 - \cos(\theta_{\mathrm{X}} - \theta_{\mathrm{O}})\right) & \frac{1}{2}\left(1 - \cos(\theta_{\mathrm{X}} - \theta_{\mathrm{O}})\right) \\ \frac{1}{2}\left(1 + \cos(\theta_{\mathrm{X}} - \theta_{\mathrm{O}})\right) & \frac{1}{2}\left(1 + \cos(\theta_{\mathrm{X}} - \theta_{\mathrm{O}})\right) \end{bmatrix} \tag{28}$$

Furthermore, Eqs. (25) and (26) reveal that the larger portion of powers from both transmitters, T1 and T2, is received by one common receiver, depending on the phase shift difference, whereas the other receiver receives the smaller power from both transmitters. The power ratios $|h_{11}|^2/|h_{21}|^2$ and $|h_{22}|^2/|h_{12}|^2$ are random and each other's inverse, and hence, their CDFs are related to one another as

$$\Pr\left[\frac{|h_{11}|^2}{|h_{21}|^2} \leq u\right] = 1 - \Pr\left[\frac{|h_{22}|^2}{|h_{12}|^2} \leq \frac{1}{u}\right] \tag{29}$$

The phenomenon that the signal from each transmitter splits in power into two received by the two receivers reveals the diversity phenomenon. This explains the MIMO capacity that nearly doubles the SISO capacity.

The above result applies to the special case where $\alpha = 0$. In reality, the orientation of the antenna pairs can be arbitrary, so that the power ratios in Eqs. (25) and (26) are also arbitrary, ranging from zero to infinity. This phenomenon differentiates the HF skywave polarized MIMO channels from the terrestrial wireless polarized MIMO channels, due to the natural presence of the X and O modes in the ionosphere.

2.3. Channel Capacity

With the above notion, we can simplify Eq. (23) further by assuming the same elevation angle for the X and O waves at both the departure and arrival. In addition, the gain patterns of the transmit and receive antennas are considered identical, so are the magnitudes of the complex path responses of the X and O modes. The only exception is the phases of the two modes, which remain different in the model.

$$\varepsilon_{\mathrm{XT}} \approx \varepsilon_{\mathrm{OT}} \approx \varepsilon_{\mathrm{XR}} \approx \varepsilon_{\mathrm{OR}} = \varepsilon$$
$$g_{\mathrm{T1}}(\varepsilon) \approx g_{\mathrm{R1}}(\varepsilon) = g_1$$
$$g_{\mathrm{T2}}(\varepsilon) \approx g_{\mathrm{R2}}(\varepsilon) = g_2$$
$$\gamma_{\mathrm{X}} \approx \gamma_{\mathrm{O}} = \gamma$$

but $\theta_{\mathrm{X}} \neq \theta_{\mathrm{O}}$. Accordingly, we obtain the simplified form of each channel matrix element as follows.

$$\begin{aligned} h_{11} &= j\frac{g_1^2\gamma}{2}[e^{j(-\alpha-\theta_{\mathrm{X}})}[\cos^2\alpha\sin^2\varepsilon + \sin^2\alpha + j\cos^2\alpha(\sin^2\varepsilon - 1)] \\ &\quad -e^{j(\alpha-\theta_{\mathrm{O}})}[\cos^2\alpha\sin^2\varepsilon + \sin^2\alpha - j\cos^2\alpha(\sin^2\varepsilon - 1)]] \end{aligned} \tag{30}$$

$$\begin{aligned} h_{12} &= j\frac{g_1g_2\gamma}{2}[e^{j(-\alpha-\theta_{\mathrm{X}})}[\cos^2\alpha(\sin^2\varepsilon - 1) + j(\cos^2\alpha + \sin^2\alpha\sin^2\varepsilon)] \\ &\quad -e^{j(\alpha-\theta_{\mathrm{O}})}[\cos^2\alpha(\sin^2\varepsilon - 1) - j(\cos^2\alpha + \sin^2\alpha\sin^2\varepsilon)]] \end{aligned} \tag{31}$$

$$\begin{aligned} h_{21} &= \frac{g_1g_2\gamma}{2}[-e^{j(-\alpha-\theta_{\mathrm{X}})}[\cos^2\alpha\sin^2\varepsilon + \sin^2\alpha + j\cos^2\alpha(\sin^2\varepsilon - 1)] \\ &\quad -e^{j(\alpha-\theta_{\mathrm{O}})}[\cos^2\alpha\sin^2\varepsilon + \sin^2\alpha - j\cos^2\alpha(\sin^2\varepsilon - 1)]] \end{aligned} \tag{32}$$

$$\begin{aligned} h_{22} &= \frac{g_2^2\gamma}{2}[-e^{j(-\alpha-\theta_{\mathrm{X}})}[\cos^2\alpha(\sin^2\varepsilon - 1) + j(\cos^2\alpha + \sin^2\alpha\sin^2\varepsilon)] \\ &\quad -e^{j(\alpha-\theta_{\mathrm{O}})}[\cos^2\alpha(\sin^2\varepsilon - 1) - j(\cos^2\alpha + \sin^2\alpha\sin^2\varepsilon)]] \end{aligned} \tag{33}$$

With the above assumptions of identical antenna patterns and homogeneous path magnitudes, we could obtain a further insight into the potential improvement of capacity achieved by this 2×2 MIMO HF channel by resorting to information theoretical definition of channel capacity:

$$C_{mn} = \log_2\left(1 + \frac{|h_{mn}|^2}{N}\right) \tag{34}$$

$$C_{\mathrm{mimo}} = \log_2\det\left(\mathbf{I}_2 + \frac{\mathbf{H}\mathbf{H}^{\mathrm{H}}}{2N}\right) \tag{35}$$

where C_{mn} denotes the SISO channel capacity between the n-th transmitter and m-th receiver, with $m,n \in \{1,2\}$; $\mathbf{I}_2$ denotes a 2×2 identity matrix; N denotes the white Gaussian noise power. The MIMO capacity in Eq. (35) is obtained by assuming orthonormal transmitted signals.

The above results demonstrate that variations in the antenna gain, polarization patterns, elevation angles of wave departure and arrival, azimuth of the path with respect to orientation of the cross-dipoles, as well as path magnitudes and phase shifts add further variations into the channel matrix elements and, subsequently, the SISO and MIMO channel capacities. In the analysis, the capacity improvement factor (CIF) is examined, which is defined as the improvement in capacity due to the MIMO configuration relative to the SISO channel of the highest capacity. That is,

$$\mathrm{CIF} = \frac{C_{\mathrm{mimo}}}{\max\limits_{m,n} C_{mn}} \tag{36}$$

It is predicted that due to the oblique propagation trajectories, there is a degradation in polarization orthogonality between antennas in the dual-antenna system employed at each end of the link, and as a result, the channel capacity improvement factor might not be as good as in the NVIS channels.

3. RESULTS

3.1. Simulation and Measurement System

The results on cross-polarization and capacity improvement in Section 2 are tested herein through simulation and measurement of an HF skywave link in the geomagnetic equatorial area of Indonesia. A dual-transmitter system is set up at the LAPAN office in Bandung ($6°53'40.1"\mathrm{S}, 107°35'12.4"\mathrm{E}$), while a dual-receiver is located in the campus of Institut Teknologi Sepuluh Nopember in Surabaya

Figure 2. The dual-transmitter and dual-receiver locations in Bandung and Surabaya.

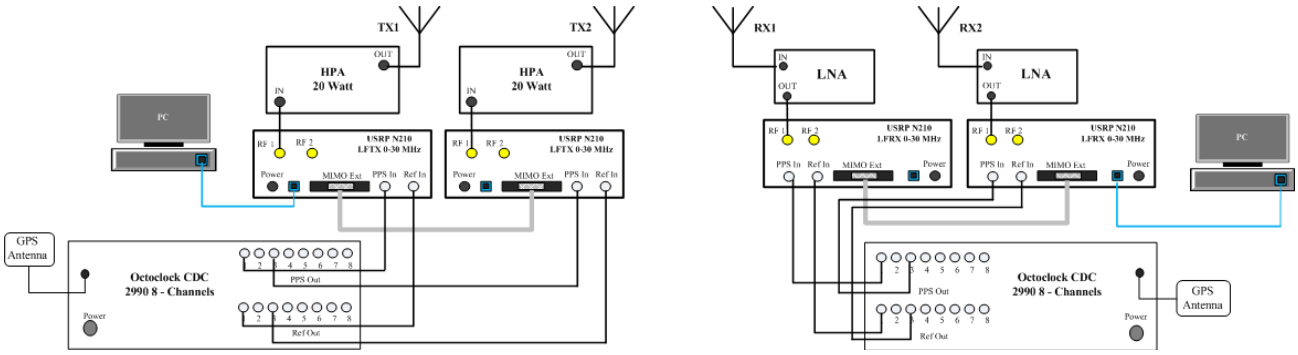

Figure 3. Block diagram of the measurement system.

(7°17′05.8"S, 112°47′46.7"E), which is approximately 575 km away to the east from Bandung. The locations of the transmitter and receiver are shown in Figure 2. Cross-dipoles are installed horizontally at a height of 12 meters at both sides of the link. The measurement system block diagram, as depicted in Figure 3, and measurement parameters used in this study have been reported in a previous paper [16]. The two transmitters emit carrier waves at different baseband frequencies, 22500 Hz and 82500 Hz, generated digitally on a software-defined radio platform of Ettus USRP N210.

Measurement is carried out on August 24–30, 2017 from 08:00 to 20:00 local time (UTC+7). The choice of carrier frequencies used during the measurement follows the daily estimation of foF2 data provided by LAPAN, which are 7 MHz for the period of 08:00–16:00 and 5 MHz for the period of 16:00 to 20.00. At the receiver, the antenna is connected to LNA with 20 dB gain. There are 5 samples recorded every 15 minutes transmission during the measurement. The result consists of 175 sets of 2×2 complex envelopes, normalized by the square root of the transmit power, at each baseband frequency.

Ionospheric ray tracing simulation is also carried out using PropLab^{TM} for the period of August 24–26, 2016. The Appleton-Hartree model of the ionospheric propagation is used, taking into account both the geomagnetic fields and electron collisions. For each of O and X modes, the phase shift is calculated by taking the remainder of division of the ray path length by the wavelength and multiplying it by 2π. Two cross-dipoles are employed at both sides, with a dipole on the East-West and the other on North-South direction for each side, leading to four combinations of transmit-receive antennas which provide a 2×2 MIMO channel. Since the Surabaya-Bandung axis is not precisely in the East-Wave direction, there is a non-zero azimuth involved in the transmitter-receiver configuration. The channel

responses for MIMO matrix element are computed using the sum of complex responses. The carrier frequencies used in the simulation are the same as those used in the measurement. The results consist of 54 samples for each matrix element.

3.2. Cross-Polarization

The CDFs of power ratios of the measured SISO channels are presented in Figure 4. Firstly, it can be observed that the CDFs of $|h_{22}|^2/|h_{21}|^2$ and $|h_{11}|^2/|h_{12}|^2$ exhibit relatively little deviation from 0 dB, as predicted by (27). Secondly, the CDFs of $|h_{11}|^2/|h_{21}|^2$ and $|h_{22}|^2/|h_{12}|^2$ fulfill the relationship given by Eq. (29). These serve as a confirmation to the earlier notions that the power contributions of T1 and T2 to the power received by each receiver are nearly identical and that the received power is more concentrated on one of the receivers. With regards to the latter, throughout the measurement campaign greater power from both transmitters is delivered to receiver R1 for approximately 80% the time, as shown by the CDF values at 0 dB of $|h_{11}|^2/|h_{21}|^2$ and $|h_{22}|^2/|h_{12}|^2$, which are 23% and 82%, respectively. This observation also confirms the split of power transmitted by any of the transmitter into both receivers, R1 and R2, albeit of different levels of power, implying the diversity phenomenon that occurs naturally.

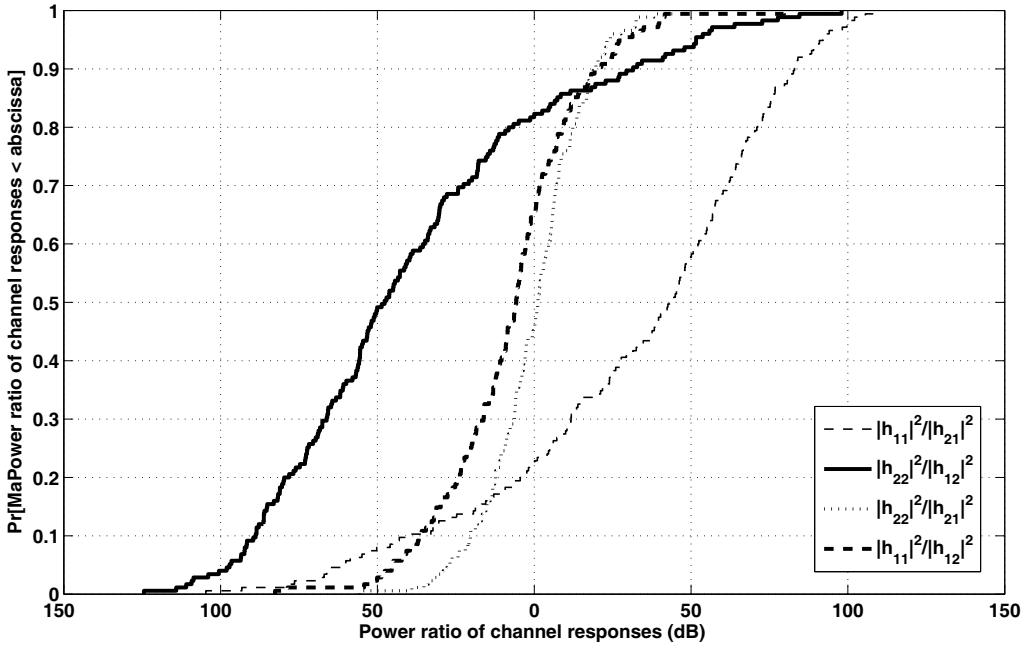

Figure 4. CDFs of the power ratios of the SISO channel responses.

3.3. SISO and MIMO Capacity

The 2×2 MIMO capacity is calculated using Eq. (35), whereas the SISO capacity is calculated using Eq. (34) for each channel element obtained from either the simulation or the measurement. The channel capacities obtained from measurement are computed using noise power N measured by the receiver when the transmitter is inactive, whereas those from the simulation are obtained by assuming a receiver noise bandwidth of 10 kHz.

The CDFs of capacity improvement factor (CIF) from both measurement and simulation can be obtained using Eq. (36). Figure 5 shows the CDFs of capacity improvement from measurement and simulation results for NVIS and oblique propagation channels. It reveals that in oblique propagation channels, the 2×2 MIMO configuration improves the capacity by a factor ranging from 1.49 to 1.79 and from 1.73 to 1.88 over the SISO capacity when the measurement and simulation results are concerned,

Table 1. Capacity improvement range of both simulation and measurement in NVIS and oblique channel.

Type of Paths	Simulation	Measurement
NVIS	1.80–1.97	1.52–1.86
Oblique	1.73–1.88	1.49–1.79

respectively, as seen in Table 1. The gap between the measurement and simulation results is due to the presence of ionospheric factors not accounted for in the simulation.

When the results for NVIS and oblique propagation channels presented in Figure 5 and Table 1 are compared, the CIF of MIMO systems in oblique propagation channels on average proves to be slightly lower than that in NVIS channels. This supports the earlier hypothesis that the oblique path trajectory reduces the polarization orthogonality between horizontal dipoles in the cross-dipoles configuration at each of the dual-transmitter and dual-receiver systems, which in turn reduces the capacity improvement.

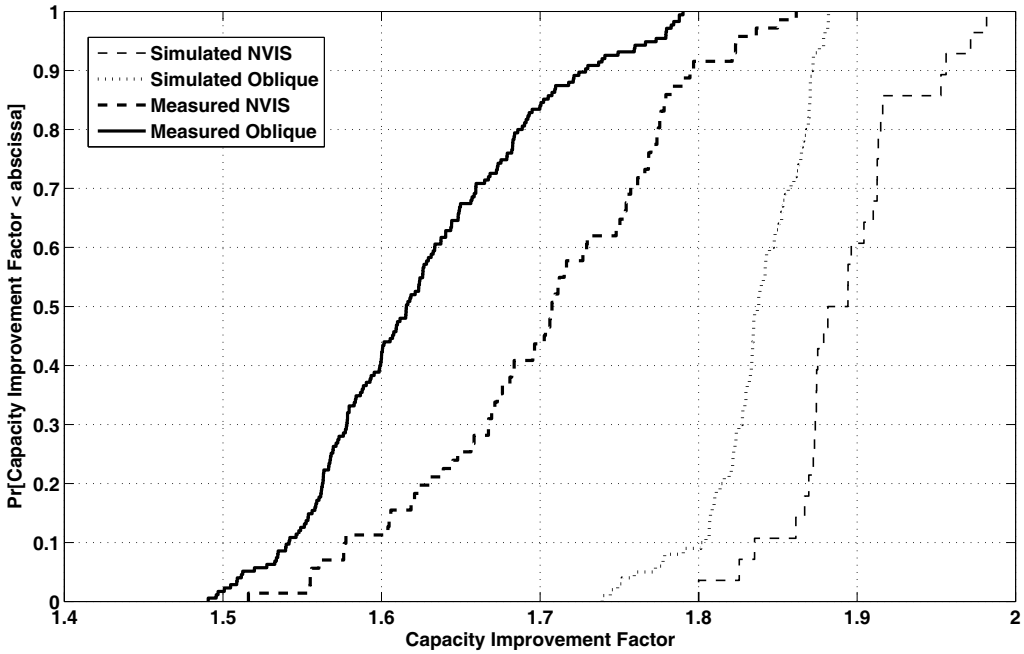

Figure 5. CDF of capacity improvement factor (CIF) of MIMO channels with NVIS and oblique paths from measurement and simulation.

4. CONCLUSION

The 2×2 HF MIMO channels on a link with oblique single-hop paths have been expressed in a mathematical form and investigated by measurement and simulation to study the phenomenon behind the channel capacity improvement by considering the role of the O and X waves in HF communications. The power transition matrix that indicates cross-polarization between the two sides of the MIMO antenna system turns out to depend on the phase shift difference between the O and X waves. It has been demonstrated in the mathematical derivation and in the measurement that the powers transmitted by the two transmitters are individually delivered in larger portion to one common receiver, whereas the other receiver receives smaller power. This indicates the occurrence of the diversity phenomenon that guarantees the capacity improvement of the 2×2 HF MIMO channels approaching twice over the SISO channel capacity. In addition, it is observed that the power received by each receiver consists of theoretically identical power contributions from the two transmitters. This has also been approximately indicated in the measurement of the power ratios of the SISO channels.

The measurement and simulation also demonstrate that on average the CIF of the 2×2 MIMO channels with oblique paths is less than that for the NVIS case. This is in line with the prediction that the oblique trajectory reduces the orthogonality of antenna polarizations in the dual-antenna system at each end of the link.

ACKNOWLEDGMENT

The reported work has been funded by Indonesian Ministry of Research, Technology and Higher Education through PMDSU scholarship to the first author as well as PREDICT 2 grant from JICA, Japan.

REFERENCES

1. Athukorala, C. P. and B. P. Resosudarmo, "The Indian Ocean tsunami: Economic impact, disaster management, and lessons," *Asian Economic Papers*, Vol. 4, No. 1, 1–39, 2005.
2. Lu, B. W., "A unified theory of ionospheric propagation of short radio waves with special emphasis on long-distance propagation," *Progress In Electromagnetics Research*, Vol. 13, 87–114, 1996.
3. ITU-R Rec. F.1761, *Characteristics of HF Fixed Radiocommunication Systems*, Intern. Telecomm. Union, Radio Sector, Geneva, Switzerland, 2006.
4. Molisch, A. F., M. Z. Win, Y. Choi, and J. H. Winters, "Capacity of MIMO systems with antenna selection," *IEEE Transactions on Wireless Communications*, Vol. 4, No. 4, 2005.
5. Shafi, M., M. Zhang, A. L. Moustakas, P. J. Smith, A. F. Molisch, F. Tufvesson, and S. H. Simon, "Polarized MIMO channels in 3-D: Models, measurements and mutual information," *IEEE Journal on Sel. Areas in Comm.*, Vol. 24, No. 3, 514–527, 2006.
6. Strangeways, H. J., "Estimation of signal correlation at spaced antennas for multi-moded ionospherically reflected signals and its effect on the capacity of SIMO and MIMO HF links," *IRST*, 306–310, London, UK, 2006.
7. Ndao, P. M., Y. Erhel, D. Lemur, and J. Le Masson, "Design of a high-frequency (330 MHz) multiple-input multiple-output system resorting to polarisation diversity," *IET Microwave Antennas Propag.*, Vol. 5, No. 11, 1310–1318, 2012.
8. Abbasi, N., "Capacity estimation of HF-MIMO systems," *IET Microwave Antennas Propag.*, *11th International Conference of Ionospheric Radio Systems and Techniques*, IRST, Edinburgh, 2009.
9. Witvliet, B. A., "The importance of circular polarization for diversity reception and MIMO in NVIS propagation," *IET Microwave Antennas Propag.*, EuCAP, The Hague, The Netherlands, 2014.
10. Erhel, Y., D. Lemur, M. Oger, J. Le Masson, and F. Marie, "Evaluation of ionospheric HF MIMO channels: Two complementary circular polarizations reduce correlation," *IEEE Antennas and Propagation Magazine*, Vol. 58, No. 6, 38–48, 2016.
11. Gunashekar, S. D., E. M. Warrington, S. M. Feeney, S. Salous, and N. M. Abbasi, "MIMO communications within the HF band using compact antenna array," *Radio Science*, Vol. 45, No. RS603, 1–16, 2010.
12. Witvliet, B. A. and R. M. Alsina-Pages, "Radio communication via near vertical incidence skywave propagation: An overview," *Telecommunication Systems*, Vol. 66, No. 2, 295–309, 2017.
13. Ndao, P. M., Y. Erhel, D. Lemur, M. Oger, and J. Le Masson, "Development and test of a trans-horizon communication system based on a MIMO architecture," *EURASIP Journal on Wireless Communications and Networking*, Vol. 2013, No. 167, 2013.
14. Enserink, S., C. Kse, M. Fitz, M. Urie, and R. McCourt, "A model for dual polarized HF MIMO communications," presented at *IEEE Military Communications Conference*, Tampa, FL, USA, Oct. 26–28, 2015.
15. Balanis, C. A., *Antenna Theory Analysis and Design*, John Wiley and Sons, New York, USA, 2005.
16. Manalu, S. L., G. Hendrantoro, and A. Mauludiyanto, "Design of measurement system for HF MIMO NVIS channel," *4th IEEE Int. Conf. on Infor. Technol., Comp., and Elect. Eng.*, Semarang, Indonesia, 2017.